

Is your inflammatory disease model falling short?

See how you can model complex human immune response and drug efficacy.



WATCH NOW

The Journal of Immunology

RESEARCH ARTICLE | FEBRUARY 15 2006

The Shaving Reaction: Rituximab/CD20 Complexes Are Removed from Mantle Cell Lymphoma and Chronic Lymphocytic Leukemia Cells by THP-1 Monocytes¹ ✓

Paul V. Beum; ... et. al

J Immunol (2006) 176 (4): 2600–2609.

<https://doi.org/10.4049/jimmunol.176.4.2600>

Related Content

Rituximab-CD20 Complexes Are Shaved from Z138 Mantle Cell Lymphoma Cells in Intravenous and Subcutaneous SCID Mouse Models

J Immunol (September,2007)

Binding of Rituximab, Trastuzumab, Cetuximab, or mAb T101 to Cancer Cells Promotes Trophocytosis Mediated by THP-1 Cells and Monocytes

J Immunol (December,2008)

Within Peripheral Blood Mononuclear Cells, Antibody-Dependent Cellular Cytotoxicity of Rituximab-Opsonized Daudi cells Is Promoted by NK Cells and Inhibited by Monocytes due to Shaving

J Immunol (August,2008)

The Shaving Reaction: Rituximab/CD20 Complexes Are Removed from Mantle Cell Lymphoma and Chronic Lymphocytic Leukemia Cells by THP-1 Monocytes¹

Paul V. Beum,* Adam D. Kennedy,* Michael E. Williams,[†] Margaret A. Lindorfer,* and Ronald P. Taylor^{2*}

Clinical investigations have revealed that infusion of immunotherapeutic mAbs directed to normal or tumor cells can lead to loss of targeted epitopes, a phenomenon called antigenic modulation. Recently, we reported that rituximab treatment of chronic lymphocytic leukemia patients induced substantial loss of CD20 on B cells found in the circulation after rituximab infusion, when rituximab plasma concentrations were high. Such antigenic modulation can severely compromise therapeutic efficacy, and we postulated that B cells had been stripped (shaved) of the rituximab/CD20 complex by monocytes or macrophages in a reaction mediated by Fc γ R. We developed an in vitro model to replicate this in vivo shaving process, based on reacting rituximab-opsonized CD20⁺ cells with acceptor THP-1 monocytes. After 45 min at 37°C, rituximab and CD20 are removed from opsonized cells, and both are demonstrable on acceptor THP-1 cells. The reaction occurs equally well in the presence and absence of normal human serum, and monocytes isolated from peripheral blood also promote shaving of CD20 from rituximab-opsonized cells. Tests with inhibitors and use of F(ab')₂ of rituximab indicate transfer of rituximab/CD20 complexes to THP-1 cells is mediated by Fc γ R. Antigenic modulation described in previous reports may have been mediated by such shaving, and our findings may have profound implications for the use of mAbs in the immunotherapy of cancer. *The Journal of Immunology*, 2006, 176: 2600–2609.

Targeting of Ags on cancer cells by mAbs has been a key strategy in cancer immunotherapy for >25 years (1–3). Targeting can lead to cell killing by a number of independent mechanisms: bound mAbs can initiate one or more signaling pathways that, depending upon the epitope or receptor that is targeted, induce necrosis or apoptosis, or inhibit cell growth (4–7). Alternatively, when mAbs remain fixed on the cell surface, they can interact with the efferent arm of the immune system and induce killing by recruiting the C system (8–14) and/or by facilitating interaction with Fc γ R on monocytes, neutrophils, or macrophages, thus promoting Ab-dependent cellular cytotoxicity (9, 15–18). However, in vivo binding of a therapeutic mAb to a cancer cell may also promote loss of the targeted Ag and bound mAb from the cell surface, an effect called antigenic modulation (2, 3, 19, 20). The result of this antigenic modulation is that the cancer cell escapes and the therapy becomes ineffective.

Monocytes and monocytic cell lines can efficiently induce antigenic modulation on certain mAb-targeted cancer cells (21, 22). Despite the capacity of monocytes and macrophages to internalize IgG-opsonized substrates (23–25), the mechanism of antigenic modulation promoted by monocytes has been generally presumed

to be due to internalization of IgG Ab/target Ag immune complexes by the cancer cells, rather than by monocytes.

The anti-CD20 mAb rituximab (RTX)³ has been used successfully in treatment of several B cell lymphomas (9, 26–32). Extensive preclinical evidence showed that it is neither internalized nor shed when bound to B cells (9, 27, 33). We recently reported that during the standard infusion of RTX in patients with chronic lymphocytic leukemia (CLL), a large fraction of B cells was rapidly cleared from the circulation after only 30 mg of RTX was infused (34). However, immediately after the total dose of ~700 mg of RTX had been infused, when the concentration of RTX in the bloodstream was quite high (>100 μ g/ml), substantial B cell recrudescence was evident. Importantly, most of the recrudescenced B cells had very low levels of CD20, and we found that CD20 had been removed from the cells rather than internalized (34).

We have now investigated loss of CD20 from B cells in an in vitro model system, using THP-1 monocytes as effector cells (35–37). Binding of RTX to several CD20⁺ cell lines or to freshly isolated B cells from CLL patients leads, in the presence of THP-1 cells, to rapid and substantial loss of RTX and CD20 from the B cell surface. However, RTX and CD20 are not internalized by the opsonized CD20⁺ cells; rather, the RTX-CD20 complexes are removed from the opsonized cells and are taken up by the THP-1 cells, in an Fc γ R-mediated process we term shaving. This shaving process may explain the enhanced antigenic modulation seen earlier in the presence of monocytes, and may explain why RTX as a single agent has had limited success in CLL treatment (27, 28, 38).

*Department of Biochemistry and Molecular Genetics and [†]Division of Hematology/Oncology and Hematologic Malignancy Program, University of Virginia School of Medicine, Charlottesville, VA 22908

Received for publication August 18, 2005. Accepted for publication November 30, 2005.

The costs of publication of this article were defrayed in part by the payment of page charges. This article must therefore be hereby marked *advertisement* in accordance with 18 U.S.C. Section 1734 solely to indicate this fact.

¹ This study was supported by the Lymphoma Research Foundation Mantle Cell Lymphoma Grant (to M.E.W.), the Commonwealth Foundation for Cancer Research (to M.E.W. and R.P.T.), and the University of Virginia Cancer Support Grant.

² Address correspondence and reprint requests to Dr. Ronald P. Taylor, Department of Biochemistry and Molecular Genetics, University of Virginia Health Sciences Center, P.O. Box 800733, Charlottesville, VA 22908-0733. E-mail address: rpt@virginia.edu

³ Abbreviations used in this paper: RTX, rituximab; 7-AAD, 7-aminoactinomycin D; AI, Alexa; CLL, chronic lymphocytic leukemia; MESF, molecules of equivalent soluble fluorochrome; MPS, mononuclear phagocytic system; NHS, normal human serum; RA, all *trans*-retinoic acid.

Materials and Methods

Cells

CD20⁺ Raji and ARH 77 cells, and THP-1 cells were obtained from American Type Culture Collection and maintained as described previously (34, 39, 40). CD20⁺ Z138 mantle cell lymphoma cells (41) were cultured in RPMI 1640 with 10% heat-inactivated FBS, 100 U/ml penicillin, 100 μg/ml streptomycin, and 2 mM glutamine. Blood was obtained from CLL patients, and mononuclear cells were isolated as described previously (34, 39). The University of Virginia Institutional Review Board approved all protocols. RTX-opsonized Raji, ARH 77, Z138, and CLL cells are designated as donor cells, and THP-1 cells as acceptor cells.

Antibodies

RTX was purchased at the University of Virginia hospital pharmacy. The mAbs 3E7 (specific for C3b/iC3b) and HB43 (specific for the Fc region of human IgG) have been described (39, 42), and were labeled with Alexa (Al) 488 or Al647 (Molecular Probes) according to the manufacturer's instructions. PE anti-CD19, PE anti-CD45, and PE anti-CD55 were from Caltag Laboratories. Anti-FcγRI (CD64) mAb 10.1 was from Caltag Laboratories, anti-FcγRII (CD32) mAb IV.3 was purified from a hybridoma from American Type Culture Collection, and anti-FcγRIII (CD16) mAb 3G8 (43) was provided by J. Edberg (University of Alabama). RTX F(ab')₂ were generated using the ImmunoPure F(ab')₂ preparation kit from Pierce, following the manufacturer's directions.

Reagents

PMA all *trans*-retinoic acid (RA), PKH 26 red fluorescent dye, protease inhibitors, and cytochalasin D were from Sigma-Aldrich. FL4 dye TO-PRO-3 iodide was from Molecular Probes, FL3 dye 7-aminoactinomycin D (7-AAD) was from BD Pharmingen, and FITC annexin V was from Caltag Laboratories. Piceattanol, PP2, PP3, wortmannin, chelerythrine, and genistein were purchased from Calbiochem.

Opsonization of cells with RTX and the shaving reaction

In our standard procedure, 10⁷ cells/ml were incubated with or without 10 μg/ml Al488 RTX or Al647 RTX in RPMI 1640 medium for 20 min at 37°C with gentle shaking. In some experiments, RTX opsonization was in the presence of 25% normal human serum (NHS) with or without 10 μg/ml mAb 3E7. Cells were washed with cold BSA/PBS before incubation with THP-1 cells. Two to 3 days before an experiment, THP-1 cells were treated with 1 μM PMA to induce differentiation (36, 37, 44) and were plated in 24-well plates, 10⁶ cells/well, in 1 ml (BD Biosciences). In some experiments, adherent THP-1 cells were labeled with PKH 26 (see below) before addition of RTX-opsonized donor cells.

To study shaving, the following four reaction conditions were used (Fig. 1): 1) 400 μl of RPMI 1640 medium alone added to an empty well; 2) 2 × 10⁵ RTX-opsonized cells in 400 μl added to an empty well; 3) 400 μl of RPMI 1640 medium alone added to a well containing 10⁶ adherent THP-1 cells; 4) 2 × 10⁵ RTX-opsonized cells in 400 μl added to a well containing

10⁶ adherent THP-1 cells (shaving). The first three conditions serve as controls for the fourth condition, the shaving sample. The plates were then centrifuged briefly to bring the cells into close proximity. After 45 min at 37°C, plates were placed on ice, and conditions 2 and 4 were quenched by addition of 2 ml of cold BSA/PBS. RPMI 1640 medium was aspirated from wells corresponding to conditions 1 and 3; then 2 × 10⁵ RTX-opsonized B cells were added to these wells, followed immediately by 2 ml of cold BSA/PBS. In most experiments, replicate wells were used for each paradigm.

Analysis of shaving

Following the incubation, donor cells were separated from THP-1 cells by gentle pipet aspiration and held on ice; THP-1 cells were then removed from the wells by vigorous pipetting. One aliquot of donor cells was probed with 10 μg/ml Al-labeled mAb HB43 for 45 min on ice to assay for residual cell-bound RTX. A second aliquot was also probed on ice for 45 min with Al488 RTX or Al647 RTX, whichever color was used in the initial opsonization step, to measure total available CD20. This reopsonization step was used to quantitate loss of CD20 caused by shaving. Cells were washed with PBS, fixed with 1% paraformaldehyde, and analyzed by flow cytometry (34). Alternatively, in some experiments, the putatively shaved cells were reopsonized with Alexa-labeled RTX of a different color than the Alexa label used in the primary opsonization. In all studies, mean fluorescence intensities were converted to molecules of equivalent soluble fluorochrome (MESF) using fluorescent beads (Spherotech) (34). THP-1 cells were distinguished from B cells based on different side scatter profiles. There was very little contamination of aspirated B cells by THP-1 cells: control experiments in which the adherent THP-1 cells were labeled with PKH 26 indicated very few of these cells were removed in the donor cell aspiration step.

RTX MESF values for cells analyzed after reopsonization with RTX allowed determination of shaving. Percentage of CD20 shaving was calculated by subtracting the RTX MESF for the experimental shaving sample (S, condition 4) from the average of the RTX MESFs for the three controls, and then dividing by the average of the MESFs for the controls. An example of this calculation, using the data in Fig. 2C, follows: control 1, 41,100 MESF; control 2, 35,900 MESF; control 3, 40,500 MESF; sample 4, 15,500 MESF. Thus, $((41,100 + 35,900 + 40,500)/3 - 15,500) / ((41,100 + 35,900 + 40,500)/3) \times 100\% = 60.4\%$.

We used similar conditions to measure shaving induced by THP-1 cells treated with RA. In this case, the THP-1 cells, which were not adherent, were labeled with PKH 26 (42), rendering them FL2⁺ and thus distinguishable from the donor cells by flow cytometry.

In fluorescent microscopy experiments, PMA-treated THP-1 cells were identified by staining with biotinylated anti-CD11b and Al594 streptavidin. Cells were examined using a BX40 fluorescent microscope (Olympus). Images were captured with a digital camera and Magnafire analysis software (34).

Use of blood-derived monocytes in the shaving reaction

Monocytes were isolated from normal human blood by Ficoll-Hypaque separation (34), followed by purification using a Miltenyi monocyte isolation kit and a Miltenyi AutoMACS magnetic cell separator (Miltenyi Biotec). These purified monocytes were then used in our standard shaving protocol in place of THP-1 cells. After the incubation, samples were quenched and the Z138 cells were separated from the monocytes using a Miltenyi B cell isolation kit.

Assessment of cell killing

After shaving, donor cells were stained with TO-PRO-3, FITC annexin V, or 7-AAD to assess the effect of shaving on cell viability (34, 45, 46). Percentage of dead cells was taken as the percentage of cells whose fluorescent intensity fell within the gate used to identify positive control ethanol-killed cells.

Inhibition of shaving

THP-1 cells were exposed to the following signal transduction inhibitors for 60 min at 37°C, before being mixed with donor cells: 5 μg/ml cytochalasin D, 15 μM PP2, 15 μM PP3, 50 μM piceattanol, 150 μM genistein, or 100 ng/ml wortmannin, or for 15 min at 37°C with 10 μM chelerythrine (47). To test for the role of THP-1-associated proteases, THP-1 cells were preincubated for 9 h with a protease inhibitor mixture that contained 2 mM 4-(2-aminoethyl)benzenesulfonyl fluoride, 1 mM EDTA, 5 mM 1,10-phenanthroline, 130 μM bestatin, 14 μM E-64, 1 μM leupeptin, and 0.3 μM aprotinin (48). Alternatively, THP-1 cells were incubated for 30 min at 37°C with 2 or 5 mg/ml human IgG or with 30 μg/ml mouse IgG2a,

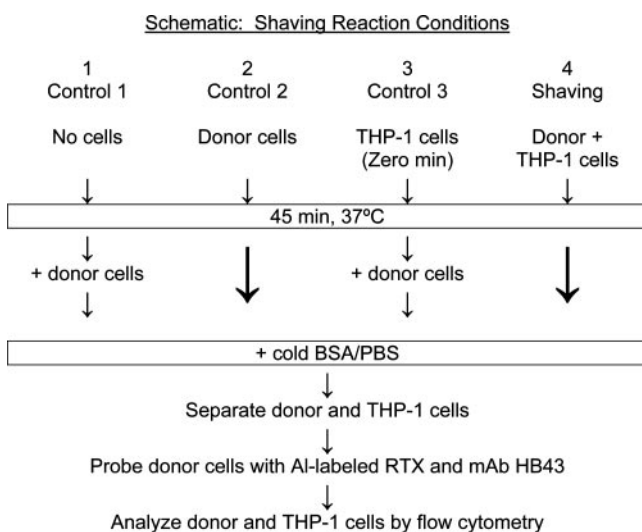


FIGURE 1. Shaving reaction conditions.

anti-Fc γ R mAbs, or mouse isotype controls. After incubation with inhibitors, THP-1 cells were used in the shaving reaction following the standard procedure with the inhibitors still present.

Western blots: tests for uptake of CD20 by THP-1 cells

Standard procedures for shaving were followed, with the exception that the two cell types were cocultured at a 1:1 ratio, to increase the amount of CD20 taken up per THP-1 cell: 1×10^6 Al488 RTX-opsonized Z138 cells were incubated with 1×10^6 PMA-treated adherent THP-1 cells. After the incubation, Z138 cells were removed from the THP-1 cells by gentle pipetting, and then the THP-1 cells were detached from the plate by vigorous pipetting and further purified by negative selection using a Miltenyi B cell isolation kit and a Miltenyi AutoMACS magnetic cell separator. Flow cytometric analysis of the purified THP-1 cells indicated $\geq 95\%$ purity of the cells. The purified THP-1 cells were lysed in 0.1 ml of 1% Triton X-100 lysis buffer containing protease inhibitors (Sigma-Aldrich P-2714), and then 50 μ g of total protein from each sample was subjected to SDS-PAGE and CD20 Western blotting (Fig. 4A and Ref. 34).

Tests for reduction of CD20 on the donor Z138 cells

Al488 RTX-opsonized Z138 cells were incubated with PMA-treated adherent THP-1 cells at the standard 1:5 ratio (Fig. 4C). After the reaction, cells were separated, further purified, and processed, as described above. Both respective isolated cell preparations were demonstrated to be $\geq 95\%$ pure when examined by flow cytometry. Tubulin Western blotting was performed to verify equal protein loading for the Z138 cells. In certain experiments, human IgG was included in the incubation mixtures to block shaving. In other experiments, the time of incubation was varied from 5 to 45 min, and then shaving of the Z138 cells and uptake of CD20 by the THP-1 cells were determined (Fig. 6B and inset).

Statistics

Means and SD were compared by *t* tests (Sigmastat; Jandel) and are displayed in Figs. 2, 3A, and 5 and in Table 1.

Results

Experimental paradigm

We developed an *in vitro* system to attempt to replicate our *in vivo* observations, which indicated that bound RTX and associated CD20 were removed from circulating B cells in CLL patients treated with the standard 375 mg/m² dose of RTX (34). Although not directly demonstrated in our previous report, we postulated that acceptor cells with Fc γ R such as monocytes or macrophages played a key role in this reaction.

To study the shaving reaction, we used as acceptor cells the human monocytic cell line THP-1, differentiated to a more macrophage-like phenotype by treatment with PMA (35–37). RTX-opsonized, CD20⁺ cells were either: 1) held on ice (control 1); 2) incubated alone at 37°C for 45 min (control 2); 3) added to THP-1 cells and immediately quenched with cold BSA-PBS (control 3, zero time); or 4) incubated with THP-1 cells at 37°C for 45 min to induce shaving (shaving sample, see Fig. 1). We used the CD20⁺ Z138 cell line, a mature B cell acute lymphoblastic leukemia line, recognized as a model for mantle cell lymphoma (41, 49, 50), for most experiments. However, to test for generality, we also exam-

ined Raji and ARH77 cells as well as primary malignant B cells from CLL patients (13, 34, 39).

Quantitative and qualitative demonstrations of shaving

As shown in Fig. 2A, Z138 cells opsonized with Al647 RTX and then incubated for 45 min at 37°C in the presence of THP-1 cells showed much greater loss of Al647 RTX (■) than did similarly opsonized cells subjected to the three control conditions (□). The modest reduction in the Al647 RTX signal for opsonized Z138 cells incubated at 37°C for 45 min in the absence of THP-1 cells (control 2) is most likely due to dissociation of bound RTX, based on its reported lability (13). The large decrease in Al647 RTX bound to the Z138 cells that were exposed to THP-1 cells is confirmed by probing these cells on ice with Al488 mAb HB43, specific for the Fc region of human IgG present in RTX (Fig. 2B, ■). Fig. 2D also shows that the Al647 RTX signal associated with the THP-1 cells increased several-fold after incubation with the Al647 RTX-opsonized cells, suggesting that much of the RTX lost by the Z138 cells was taken up by the THP-1 acceptor cells. As the acceptor THP-1 cells were in 5-fold excess over the donor Z138 cells, the fact that a considerably lower signal is found on the THP-1 cells is not unexpected.

These experiments demonstrate transfer of RTX from Z138 cells to THP-1 cells, but they do not directly reveal whether CD20 was also removed from Z138 cells along with RTX. Therefore, we examined the ability of the Z138 cells to bind additional Al647 RTX after shaving. If THP-1 cells merely removed RTX and left CD20 intact on the donor Z138 cells, the Z138 cells should still be able to bind as much RTX as control Z138 cells that had not been exposed to THP-1 cells. We incubated isolated Z138 cells, obtained from each of the three controls and the shaving condition, with additional Al647 RTX on ice. The ability of the postshaving, previously opsonized Z138 cells to bind Al647 RTX in this second opsonization step was greatly reduced (■, Fig. 2C) compared with the controls, suggesting that CD20 was removed along with the RTX. From these results, we can calculate (as illustrated in *Materials and Methods*) the percentage of CD20 shaved from the Z138 cells by comparing the MESF signals for Al647 RTX on the reopsonized postshaving Z138 cells with the average of the MESF signals for RTX on the three reopsonized control samples. Table I gives the calculated percentage of CD20 shaving for naive (non-opsonized) Z138 cells and RTX-opsonized Z138 cells (Expt. 1, based on Fig. 2), along with the results of a duplicate experiment performed 1 day later (Expt. 2). The percentage of CD20 shaving for RTX-opsonized Z138 cells, 61–76%, is representative of a total of 37 similar experiments, in which the percentage shaved was

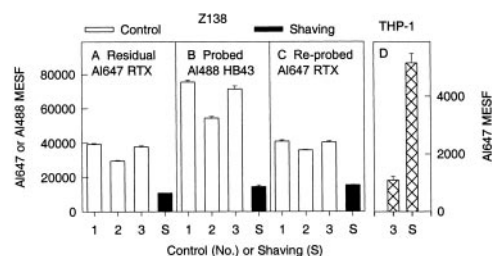


FIGURE 2. Flow cytometric analysis of shaving of RTX-opsonized donor Z138 cells by PMA-treated THP-1 acceptor cells. Al647 RTX-opsonized Z138 cells were incubated \pm THP-1 cells, separated, and analyzed under conditions, as defined in *Materials and Methods*. A, Residual donor cell-bound Al647 RTX after shaving. B, Binding of Al488 HB43 to donor cells after shaving. C, Binding of additional Al647 RTX after shaving. D, Uptake of Al647 RTX by THP-1 cells for control condition 3, or for shaving (S, condition 4). All samples were tested in duplicate.

Table 1. Percentage of CD20 shaving of RTX-opsonized cells

| Experiment | Donor Cell | Opsonization | THP-1 Treatment | % CD20 Shaving (mean \pm SD) ^a |
|------------|------------|--------------|-----------------|---------------------------------------------|
| 1 | Z138 | None | PMA | 3 \pm 0.7 |
| 1 | Z138 | RTX | PMA | 61 \pm 0.7 |
| 2 | Z138 | None | PMA | 4 \pm 2 |
| 2 | Z138 | RTX | PMA | 76 \pm 3 |
| 3 | Raji | RTX | PMA | 51 \pm 3 |
| 3 | Raji | RTX | RA | 45 \pm 2 |

^a All experiments were performed in duplicate.

70 ± 11%. Table I also shows that only ~4% shaving occurred on naive Z138 cells. In fact, in a total of 32 other shaving experiments using naive Z138 cells, we found that CD20 was not appreciably removed by THP-1 cells (3 ± 11%, *n* = 32, range from -22 to 15%). Finally, in a pilot study, human monocytes (see *Materials and Methods*) were tested for their potential to promote shaving. Under our standard shaving reaction conditions, freshly isolated human monocytes induced 73 ± 2% loss of CD20 from Al488 RTX-opsonized Z138 cells.

To provide an additional orthogonal test for loss of CD20 from RTX-opsonized cells, we first opsonized Z138 cells with Al488 RTX, and after the shaving reaction the cells were reprobbed with RTX conjugated with a second fluorochrome, Al647. The Al488 RTX signal decreased from 120,000 ± 2,000 MESF before shaving to 26,000 ± 2,000 MESF after shaving. When the cells were secondarily probed with Al647 RTX (a different preparation than that used in Fig. 2), uptake of the probe corresponded to 470 MESF for the shaved cells, and to 900 MESF for the unshaved control Al488 RTX-opsonized cells, compared with 12,200 MESF for naive Z138 cells. The low level of additional binding of Al647 RTX to the unshaved control cells is most likely due to blockade of CD20 by previously bound Al488 RTX. The shaved cells had only approximately one-fifth as much Al488 RTX bound as the control unshaved cells, but they took up even less of the secondary Al647 RTX probe, indicating that they had indeed lost the CD20 target.

We next studied the shaving process using fluorescent microscopy. We opsonized Z138 cells with Al488 RTX and then incubated them with PMA-treated THP-1 cells at 37°C for 45 min. The Z138 cells were removed, and fluorescent images of Z138 cells before and after shaving were compared. Fig. 3, *A* and *B*, shows that the intensity of the Al488 RTX signal on the Z138 cells is greatly diminished following the shaving reaction. We stained the THP-1 cells red using biotinylated anti-CD11b, followed by Al594 streptavidin (Fig. 3*E*), and when viewed through a green filter, the two THP-1 cells show a distinct green color, illustrating uptake of Al488 RTX (Fig. 3*C*). A third cell can also be seen in Fig. 3*C*, which is not visible in Fig. 3*E*. This cell is negative for CD11b, but positive for Al488 RTX, indicating that it is a Z138 cell that remained associated with the THP-1 cells. Finally, Fig. 3*D* shows the overlap of the red and green signals, revealing the presence of the green RTX within or on the red THP-1 cells.

To directly and unambiguously demonstrate transfer of CD20 from RTX-opsonized Z138 cells to THP-1 cells, we performed immunoblotting on whole cell lysates of THP-1 cells obtained before and after incubation with Al488 RTX-opsonized Z138 cells. Fig. 4*A* clearly demonstrates the presence of CD20 in the THP-1

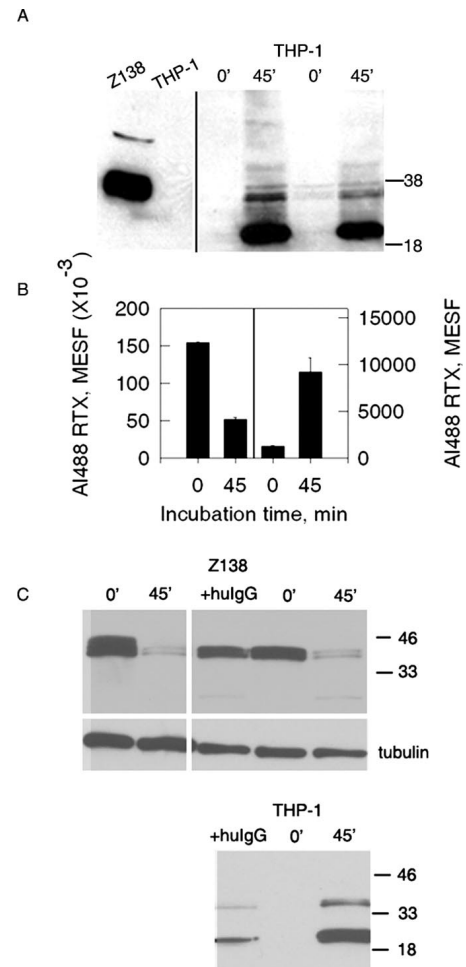


FIGURE 4. As a consequence of the shaving reaction, CD20 is transferred to THP-1 cells and removed from Z138 cells. *A*, Western blots of whole cell lysates of naive Z138 cells, naive THP-1 cells, and replicates of THP-1 cells for: 0', zero time (control 3); 45', after shaving of RTX-opsonized Z138 cells. *B*, Flow cytometry results show the Al488 RTX MESF values for the Z138 and THP-1 cells from *A* before and after shaving. *C*, *Top gel*, left to right, Western blots for CD20 of whole cell lysates of Z138 cells: 0', zero time control; 45', after shaving; separate experiment, +huIgG, 45' after coincubation of cells in the presence of 2 mg/ml human IgG; 0', 45', as before. *Middle gel*, Tubulin loading control for the *top gel*. *Bottom gel*, Western blots for CD20 of whole cell lysates of THP-1 cells for the second experiment in the *top gel*. In all experiments, the THP-1 and Z138 cells were carefully separated by aspiration, followed by purification with magnetic separation.

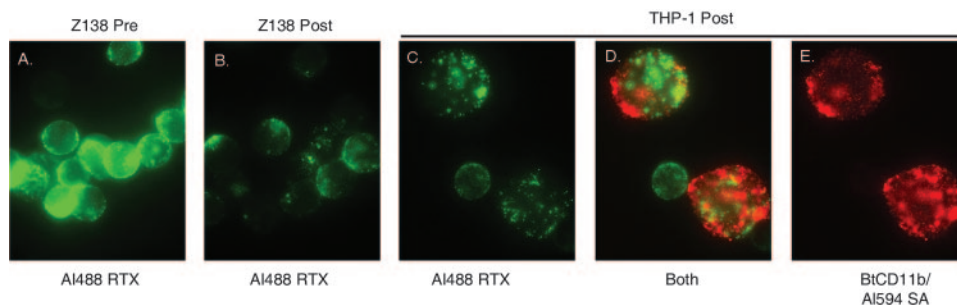


FIGURE 3. Fluorescent micrographs demonstrating CD20 shaving. Al488 RTX-opsonized Z138 cells before (*A*) and after (*B*) shaving by PMA-treated THP-1 cells. The exposure time in *A* and *B* was identical. *C–E*, Following shaving, acceptor THP-1 cells were labeled red with biotinylated CD11b and Al594 streptavidin. *C*, Green filter shows cell-associated Al488 RTX; *D*, simultaneous red and green filters show both the Al488 RTX and the red THP-1 cells; *E*, red filter shows the THP-1 cells. Original magnification: ×100.

cells after, but not before, the shaving reaction. The lower m.w. bands in Fig. 4A most likely represent degraded fragments of internalized CD20 taken up by the THP-1 cells. Consistent with the Western blotting results, flow cytometry analyses (Fig. 4B) confirm that A1488 RTX was taken up by the THP-1 cells and that the Z138 cells had suffered a substantial loss of A1488 RTX.

The quantitative findings in the flow cytometry experiments demonstrate that >70% of both RTX and CD20 are removed from the Z138 cells. To independently test for CD20 loss from these cells, we performed Western blotting on Z138 cells before and after the shaving reaction, and we included loading controls, based on tubulin staining, to validate the comparison. Fig. 4C shows two independent experiments that demonstrate that most CD20 was removed from the Z138 cells. Furthermore, we find that human IgG inhibits shaving of CD20, which will also be demonstrated in more detail in a later experiment (Fig. 8 below). Finally, Western blots reveal a reciprocal relationship between the CD20 content of Z138 and THP-1 cells. In the 45-min shaving samples (*fifth column*, Fig. 4C), large amounts of CD20 are associated with the THP-1 cells, whereas little CD20 is found with the Z138 cells. However, in the sample inhibited with human IgG, and in the zero time control sample (*third and fourth columns*, Fig. 4C), most of the CD20 remains associated with the Z138 cells.

Parameters affecting shaving

THP-1 cells can also be induced to undergo differentiation into a more macrophage-like state by treatment with retinoic acid (36, 37, 44), and, as illustrated in Table I, Expt. 3, THP-1 cells promoted comparable levels of shaving of RTX-opsonized Raji cells after differentiation with either PMA or retinoic acid. We also found that PMA-treated adherent THP-1 cells were able to remove RTX and CD20 from ARH77 cells (Fig. 5A). Moreover, although the degree of shaving was lower in some cases, freshly isolated cells from several patients with CLL, opsonized *in vitro* with RTX, also underwent CD20 shaving when incubated with RA- or PMA-treated THP-1 cells (Fig. 5A).

We considered the specificity of the CD20 shaving reaction, i.e., whether it promoted indiscriminate removal of cell surface markers or whether it was specific for CD20. To address this question, following the shaving reaction, we probed Z138 cells for CD20, CD19, CD45, and CD55. Although the latter three markers were partially removed, loss of these markers was far less than the loss observed for CD20 (Fig. 5B). It is possible that certain proteins, e.g., CD19, perhaps located in close proximity to the CD20-RTX complex, were partially removed as innocent bystanders when the RTX-CD20 complexes were shaved.

Opsonization of CD20⁺ cells with RTX in the presence of NHS leads to substantial deposition of C3b and its fragments on the cells, with much of the deposited C3b in close proximity to cell-bound RTX (34, 39). We therefore asked whether deposited C3b might affect the degree of shaving, either by blocking access of FcγR, which might lead to less shaving, or by interacting with CR1 or CR3 on the THP-1 cells, which would be expected to enhance interaction between the Z138 and THP-1 cells. However, Fig. 5C shows that opsonizing Raji or Z138 cells with A1488 RTX in the presence of NHS (followed by multiple washes) does not markedly affect the degree of CD20 shaving compared with that observed when cells were opsonized with RTX in medium. Furthermore, addition of mouse IgG1 anti-C3b mAb 3E7, which binds to and stabilizes C3b and iC3b during C activation on the cells (51), had little influence on the shaving reaction (Fig. 5C).

As shown in Table I, naive Z138 cells demonstrate little loss of CD20 when they are incubated with THP-1 cells, and we next investigated how the degree of opsonization of the cells with RTX

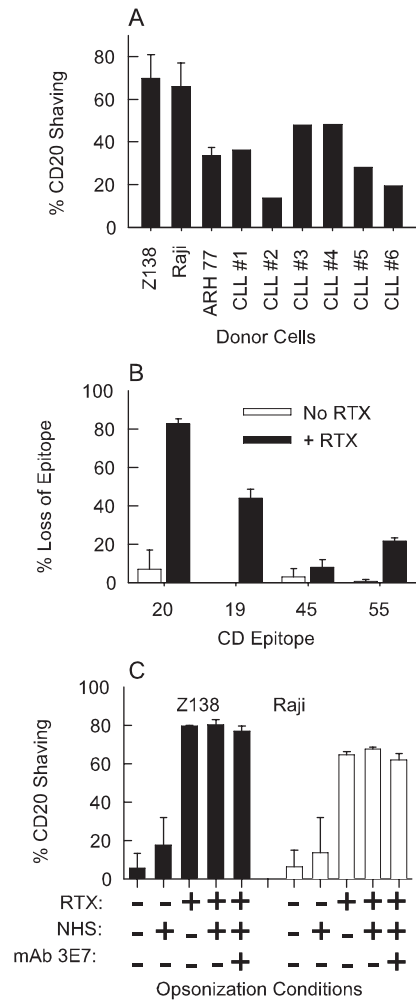


FIGURE 5. Parameters affecting CD20 shaving. *A*, Three different CD20⁺ cell lines (Z138, *n* = 37; Raji, *n* = 8; ARH77, *n* = 2) or Ficoll-isolated B cells from six different CLL patients were opsonized with RTX, and then subjected to shaving with either PMA-treated THP-1 cells (Z138, Raji, CLL patient 1) or RA-treated THP-1 cells (ARH 77, CLL patients 2–6). *B*, Naive or RTX-opsonized Z138 cells were incubated with PMA-treated THP-1 cells, then probed with Abs against the indicated CD markers (*n* = 2). *C*, Z138 and Raji cells were opsonized with various combinations of RTX, 25% NHS, and mAb 3E7; washed thoroughly; and then incubated with PMA-treated THP-1 cells in a standard shaving reaction (*n* = 2).

influenced the level of shaving (Fig. 6A). The dose response for the experiment indicates that more shaving occurs when more RTX is used to opsonize the cells, and in fact at an initial concentration of 10 μg/ml, approximate saturation with respect to both RTX binding and shaving is evident. Fig. 6A was fit to a simple binding isotherm model, and gives a *K_D* for RTX binding to CD20 on Z138 cells of 1.3 nM, which is in reasonably good agreement with the reported results of direct binding studies (52). We next examined the kinetics of the shaving reaction (Fig. 6B). The reaction is substantially complete at 45 min, the usual time for our assays. In one of the two experiments illustrated in Fig. 6B, we isolated the THP-1 cells and then performed Western blotting on the cells to test for uptake of CD20. The *inset* in Fig. 6B reveals that as the shaving reaction proceeds (0–15 min), increasing amounts of CD20 are taken up by the THP-1 cells, and at later times the CD20 appears to be processed and degraded to smaller fragments, consistent with internalization of CD20 by the THP-1 cells. Finally, Fig. 6C demonstrates that when the THP-1 cells are

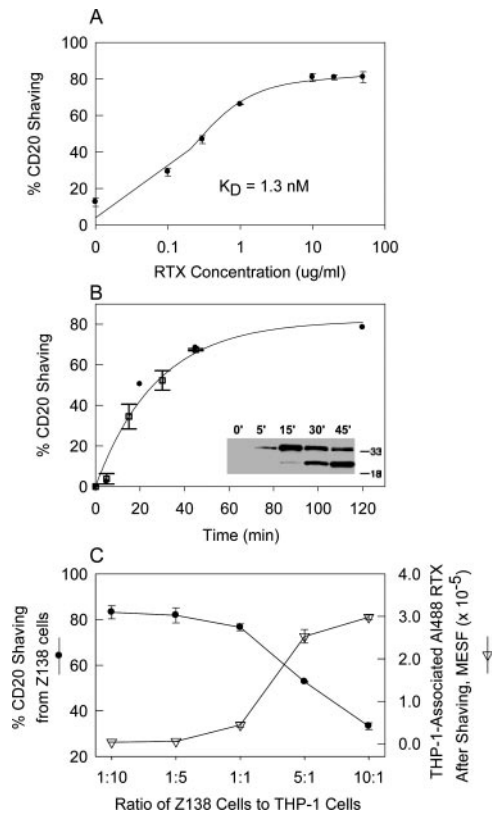


FIGURE 6. Dependence of CD20 shaving on RTX concentration, incubation time, and cell ratios. *A*, Influence of Al488 RTX opsonization concentration ($n = 2$, each point). *B*, Kinetics of shaving for the standard shaving protocol. Two separate experiments are shown, and the data were fit to a single exponential rise, with a $t_{1/2}$ of 19 min. In the second experiment, in which error bars denote duplicate points, Western blots in the *inset* illustrate uptake of CD20 by the THP-1 cells. *C*, Combinations of RTX-opsonized Z138 cells and THP-1 cells were tested in the shaving reaction at cell ratios varying between 1:10 and 10:1. Donor cells were assayed for shaving, and acceptor THP-1 cells were examined for uptake of Al488 RTX ($n = 2$, each point).

in relative excess over Z138 cells, the Z138 cells experience a high level of shaving, but the amount of Al488 RTX taken up per THP-1 cell is quite low, because the amount of Al488 RTX substrate is limiting. Alternatively, when Z138 cells are in excess, the degree of shaving per donor cell is modest, but each THP-1 cell takes up much more Al488 RTX (Fig. 6C).

Effect on cell viability

We examined the effect of CD20 shaving on the viability of the B cells, because if the shaving reaction is able to kill the B cells, then this process might not reduce the efficacy of RTX therapy. However, as shown in Fig. 7, based on three different indicators of cell viability, we saw no significant increases in apoptosis or in cell death caused by the shaving reaction.

Exploration of mechanism

To examine mechanism(s) by which THP-1 cells remove bound RTX and CD20 from B cells, we pretreated THP-1 cells with two groups of inhibitors. One group targets signaling pathways known to be involved in phagocytosis (47). These inhibitors can therefore provide information as to whether phagocytosis and shaving are governed by similar processes. Fig. 8A shows that cytochalasin D was able to block the shaving reaction very effectively. This inhibitor interferes with actin filament formation, showing that this

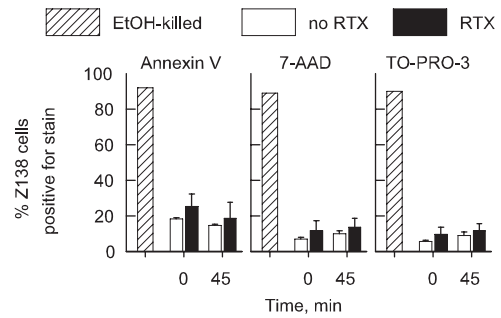


FIGURE 7. Effect of CD20 shaving on cell viability. Naive or RTX-opsonized Z138 cells were incubated with PMA-treated THP-1 cells; then the Z138 cells were isolated, stained with either 1 $\mu\text{g/ml}$ FITC annexin V, 2 $\mu\text{g/ml}$ 7-AAD, or 1 μM TO-PRO-3 iodide, and analyzed by flow cytometry ($n = 2$).

process is crucial for the shaving reaction. Interestingly, however, none of the inhibitors that block specific signaling pathways important for phagocytosis (47) was able to inhibit shaving, showing that shaving and phagocytosis are mechanistically distinct. Finally, we found that a protease inhibitor mixture blocked shaving (Fig. 8A), suggesting that a proteolytic step is involved in the shaving reaction.

The other set of inhibitors we used are Abs that can bind to Fc γ RI, II, and III on the THP-1 cells. In agreement with Fig. 4C, pretreatment of THP-1 cells with human IgG inhibited shaving (Fig. 8B), suggesting an important role for Fc γ R, which should recognize the human IgG1 portion of RTX. Moreover, an irrelevant mouse IgG2a mAb, an isotype that is known to bind with high affinity to Fc γ RI (53), also blocked shaving. Use of a mAb that specifically blocks Fc γ RI function inhibited shaving $\sim 35\%$, while use of blocking mAbs specific for the other two major Fc γ Rs, either alone or in a mixture, had no effect on the degree of shaving. These results suggest that Fc γ RI, which binds human IgG1 and mouse IgG2a with high affinity, may be the primary THP-1 receptor important for the shaving reaction.

We directly tested for the importance of the Fc portion of RTX by preparing F(ab')₂ of the mAb. Fig. 8C indicates that there is little, if any, shaving of donor Z138 or Raji cells by THP-1 cells when the donor cells are opsonized with the F(ab')₂ of RTX, further supporting the importance of an Fc γ R-mediated process for the shaving reaction. Differences between no RTX and Al488 RTX F(ab')₂ were not statistically significant ($p = 0.25$ and 0.14 , respectively, for Z138 and Raji cells), but differences for intact RTX vs no RTX were significant ($p = 0.002$ and 0.01 , respectively).

We have already demonstrated that shaving of CD20 occurs in vivo, and this finding implies that human IgG in the bloodstream (~ 10 mg/ml) does not block shaving. To address this question in our in vitro model, we tested the ability of NHS or heat-inactivated NHS to block the shaving reaction. In a representative experiment ($n = 3$), we observed the same amount of shaving in buffer ($86 \pm 1\%$) as in 50% NHS ($85 \pm 1\%$). Thus, our in vitro model replicates the observation in vivo. Finally, when the NHS was first heat inactivated, shaving decreased to $43 \pm 2\%$, which was comparable to the amount of shaving observed when 5 mg/ml human IgG was added to the shaving reaction mixture buffer ($43 \pm 5\%$).

If fixed tissue macrophages in liver and spleen play a role in shaving in vivo, then multiple passes of an RTX-opsonized cell through these organs could lead to consecutive increases in shaving. Indeed, we found that B cells that had undergone $68 \pm 1\%$ shaving after one incubation with THP-1 cells were shaved a total of $80 \pm 0.1\%$ after reopsonization with RTX and a second incubation with fresh THP-1 cells ($p = 0.004$, $n = 2$).

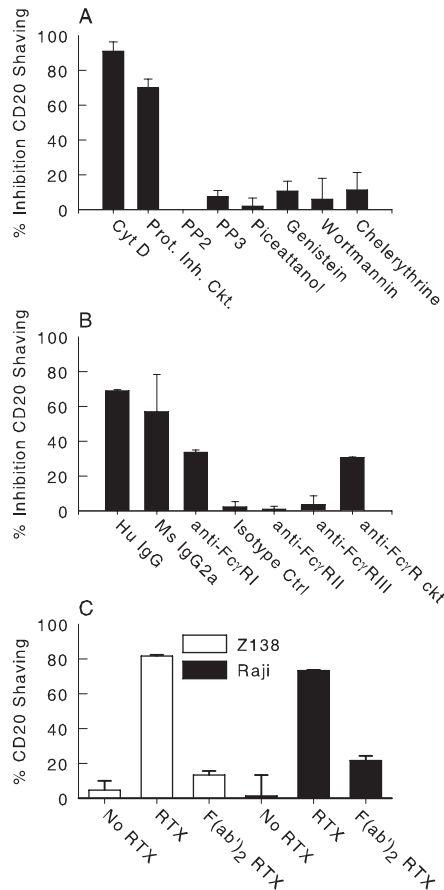


FIGURE 8. Inhibition of CD20 shaving. *A* and *B*, PMA-treated THP-1 cells were pretreated with the indicated inhibitors (for concentrations, see *Materials and Methods*) and then tested for their ability to promote shaving of A1488 RTX-opsonized Z138 cells ($n = 2$). Isotype control: mouse IgG1 for anti-Fc γ RI. Anti-Fc γ R ckt, mixture: 30 μ g/ml each anti-Fc γ R mAb. *C*, Z138 and Raji cells were opsonized with nothing, 10 μ g/ml A1488 RTX, or 10 μ g/ml A1488 RTX F(ab')₂, and then incubated with THP-1 cells under standard conditions ($n = 2$). After separation, naive cells were opsonized with intact RTX, and the putatively shaved donor cells were reopsonized with the same mAb used in the first opsonization step.

It is possible that phagocytosis, rather than shaving, could explain some of our findings. Therefore, we analyzed flow cytometry data from 39 independent shaving experiments on 12 separate days to measure the quantitative recovery of RTX-opsonized donor cells after the standard 45-min incubation. Compared with the 0-min RTX-opsonized control (control 3), $74 \pm 17\%$ of RTX-opsonized cells were recovered. It is likely that one of the reasons for the lack of full recovery is due to continued adherence of some donor cells to THP-1 cells (Fig. 3, *C* and *D*). Moreover, visual inspection of fields of adherent THP-1 cells after shaving failed to reveal any obviously phagocytosed cells. Also, we incubated either naive or RTX-opsonized Z138 cells with THP-1 cells for periods up to 8 h. In a representative 8-h experiment, we observed greater recovery of RTX-opsonized Z138 cells ($82 \pm 7\%$) than of naive Z138 cells ($66 \pm 9\%$, $p = 0.18$, $n = 2$), providing additional evidence that there was little phagocytosis of the RTX-opsonized cells under the conditions of these studies.

Discussion

Shaving is readily demonstrable

Incubation of acceptor THP-1 cells with four different types of RTX-opsonized donor cells, including B cells from CLL patients,

promoted rapid removal of a large fraction of bound RTX and CD20 from the opsonized cells (Figs. 2–6). Our experiments suggest that the RTX/CD20 complex was shaved from donor cells and transferred to THP-1 cells in a concerted reaction. The key observation supporting this conclusion is that, during the reopsonization step, we observed very little binding of additional RTX to the donor cells following shaving, indicating an absence of available, nonligated CD20 on the donor cells (Fig. 2*C*). Furthermore, Western blotting experiments (Fig. 4, *A* and *C*, and 6*B*) directly demonstrated that CD20 fragments were associated with the acceptor THP-1 cells after the shaving reaction.

It is possible that some phagocytosis of the donor cells occurred during the shaving reaction. However, cells were incubated together for only 45 min, and comparable studies suggest that little phagocytosis would occur in such a short time (54, 55). Furthermore, $\sim 75\%$ of the input RTX-opsonized donor cells were recovered after a typical shaving reaction. Considering that the ratio of THP-1 cells to donor cells used in our experiments was usually 5:1, this would mean that, at most, ~ 5 donor cells would be phagocytosed for every 100 acceptor THP-1 cells. It is quite possible, in fact, that donor cells lost during the shaving reaction were not phagocytosed, but remained adhered to the THP-1 cells (Fig. 3).

Control experiments indicated that naive nonopsonized CD20⁺ cells do not lose appreciable amounts of CD20 upon incubation with THP-1 cells (Table I; Figs. 5, *B* and *C*, and 6*A*). Dose-response experiments provided additional evidence that donor cell-bound RTX is indeed required to induce shaving, and that shaving reached approximate saturation when cells were opsonized with a 10 μ g/ml input of RTX (Fig. 6*A*). The results in Fig. 6*A* support the hypothesis that use of lower doses of RTX to treat CLL patients may lead to reduced amounts of shaving, a concept that has been validated in a pilot clinical trial (56). We also found that comparable amounts of shaving were demonstrable in the presence and absence of NHS. This result is consistent with our *in vivo* observations that shaving of RTX-CD20 complexes from B cells does indeed occur in the body, despite the presence of endogenous human IgG in the bloodstream and in most extracellular fluids. Serum that is heat inactivated does block shaving, and several complement components that can interact with IgG, including C1q, C3, and C4 (57–61), are denatured by heat inactivation. These results suggest that one or more of these complement proteins may modulate the binding of IgG or cell-bound RTX to Fc γ RI (34, 39, 62).

Role of Fc γ R in the mechanism of shaving

Our *in vitro* studies indicate that Fc γ R play a role in the shaving reaction. First, shaving is abrogated when F(ab')₂ of RTX are used in place of the intact mAb (Fig. 8*C*). Second, THP-1 cells express high levels of Fc γ RI and II (63, 64); human IgG, heat-inactivated NHS, and mAbs that bind to Fc γ RI (but not to Fc γ RII) inhibit shaving (Fig. 8*B*). These results therefore suggest that Fc γ RI may be the key receptor involved in the shaving reaction.

The detailed mechanism of the shaving reaction most likely differs considerably from that of phagocytosis, and in fact it shows more features in common with endocytosis. Cytochalasin D, an inhibitor of actin filament formation known to block phagocytosis and some forms of endocytosis (65), also inhibited the shaving reaction. However, shaving was not blocked by tyrosine kinase inhibitors known to block phagocytosis (Fig. 8*A*) (47). Phagocytosis is characterized by sequential phosphorylation of cellular proteins mediated by Src and Syk kinases (66), whereas simple endocytosis of small Ab-Ag complexes does not require tyrosine kinase action (23). Based on these considerations, we propose the following mechanism for shaving.

After the donor cell is opsonized with RTX, it is brought into close juxtaposition with the acceptor cell, based on recognition of bound RTX by Fc γ RI on the acceptor cell, thus forming an immunological synapse (65, 67). Small regions of membrane fragments containing RTX/CD20 complexes are then pinched off the RTX-opsonized donor cell and internalized by the acceptor monocyte/macrophage. This process, a type of endocytosis, is called trogocytosis, and has been described for T and B lymphocytes and for NK cells (67–69). In trogocytosis, target cell-derived molecules (on the donor cell) including the Ag itself are captured, probably via receptor-mediated internalization (by the acceptor cell) (69). In their studies of bispecific Ab-mediated phagocytosis of targeted cells, Wallace et al. (55) reported that macrophages appeared to be chipping away at the target cells; this phenomenon may also reflect the trogocytosis mechanism we have proposed for the RTX/B cell/THP-1 system. Monocytes and macrophages express a number of proteases on their surfaces (70, 71), and the shaving process is likely to include a proteolytic step, and indeed the reaction was inhibited by a protease inhibitor mixture (Fig. 8A).

Relevance of shaving to RTX therapy for CLL

Taken as a whole, these in vitro findings recapitulate our previous in vivo investigations of the fate of CD20 on circulating B cells when patients with CLL were treated with the standard 375 mg/m² dose of RTX. That is, most of the CD20 was removed, and presumably cells could then persist in the circulation despite the presence of high levels of RTX, because the shaved cells could no longer be opsonized with RTX and therefore escaped recognition as targets for immune clearance (34).

Loss of CD20 from circulating B cells does not appear to occur when patients with low B cell burdens are treated with RTX (26–28, 72, 73). Under these conditions, it is likely that the capacity of effector cells of the mononuclear phagocytic system (MPS), expressing Fc γ RII and Fc γ RIII (15, 74–76), is sufficient to take up and destroy the RTX-opsonized cells. However, infusion of the standard dose of RTX in CLL patients with high circulating B cell burdens is likely to lead to saturation of the cellular clearance mechanisms mediated by the MPS (43). That is, the large number of RTX-opsonized cells may overwhelm the most immediate clearance and killing capacity of the MPS, and under these conditions a secondary reaction occurs: the shaving of RTX-CD20 complexes from the highly opsonized B cells (34, 77, 78). It is likely that shaving is mediated by cellular Fc γ RI (53), which, despite the level of competing monomeric IgG in the circulation, can interact effectively with opsonized B cells containing large amounts of bound RTX. These effector cells may include both fixed cells, such as Kupffer cells and liver endothelial cells, as well as circulating monocytes (23, 24, 79).

Shaving as a mechanism for antigenic modulation: historical perspective

Shaving appears to be quite similar to the phenomenon of antigenic modulation, that is, loss of a tumor cell target Ag induced by binding of a mAb (2, 3, 19–22, 80). The mechanism of shaving, which may underlie many cases of antigenic modulation, includes transfer of mAb and tumor cell Ag to the acceptor monocyte/macrophage, rather than internalization of Ag by the target cell. In certain cases, such internalization (in the absence of monocytes) has clearly been documented (81), but often the reaction requires or is enhanced by accessory cells expressing Fc γ RI (21, 22, 80, 82, 83). In fact, our observations bear striking similarities to the reports of Schroff et al. (21, 22), who studied antigenic modulation induced by mAb T101 on a lymphocyte membrane-associated Ag (T65), now recognized as CD5 (84). The mAb caused moderate

antigenic modulation in isolated purified lymphocytes. However, THP-1 cells and monocytes substantially enhanced antigenic modulation mediated by mAb T101, and we have confirmed that these effector cells promote CD20 shaving in the present system. These investigators demonstrated that mAb T101-mediated antigenic modulation also required the Fc region of mAb T101, as we find for RTX. We suggest that the T101 mAb and T65 Ag (CD5) were transferred to acceptor monocytes. Consistent with this postulate, Schroff et al. (21) recognized that antigenic modulation occurred to a far lower degree in vitro than in vivo, and suggested that macrophages in the liver and lungs were responsible for the higher level of in vivo antigenic modulation. Several other investigators have reported similar evidence for antigenic modulation in other systems (2, 20, 80, 82, 83). However, to our knowledge, no one has investigated mechanisms based on Fc γ R-mediated transfer of mAbs and targeted Ags from tumor cells to acceptor monocytes/macrophages.

Implications of shaving for the use of mAbs in cancer immunotherapy

The distinction between internalization by the tumor cell vs transfer to an acceptor monocyte/macrophage has profound implications for cancer immunotherapy. For example, several immunotherapeutic mAbs are coupled to cytotoxic agents for intracellular delivery to tumor cells (81, 85); therapies based on these constructs could fail or promote serious side effects if, after such reagents bound to the tumor cell, they were instead transferred to and internalized by acceptor monocytes/macrophages, thus inducing damage to Fc γ R-expressing cells in the liver (86) or in other organs.

One issue to address is how to preserve cell killing mechanisms while reducing or eliminating shaving. First, substantially lower, but more frequent doses of RTX may enhance B cell killing and decrease shaving in CLL (56). Second, several investigations have demonstrated that polymorphisms in Fc γ RII and Fc γ RIII reliably predict the best response to RTX for B cell lymphomas other than CLL (74–76, 87). Thus, selective blockade of Fc γ RI may be sufficient to inhibit shaving induced by RTX without impairing the therapy. Future therapeutic approaches might include use of either a specific blocking mAb or other reagents that inhibit processes mediated by Fc γ RI, but that preserve the cytotoxic actions of RTX mediated by C and by Fc γ RII and Fc γ RIII.

We have begun to investigate the shaving reaction for other mAbs currently in use or under investigation for cancer immunotherapy. If our findings can be generalized to these other systems, the shaving reaction may have major implications for the immunotherapy of cancer.

Disclosures

The authors have no financial conflict of interest.

References

- Nadler, L. M., P. Stashenko, R. Hardy, W. D. Kaplan, L. N. Button, D. W. Kufe, K. H. Antman, and S. F. Schlossman. 1980. Serotherapy of a patient with a monoclonal antibody directed against a human lymphoma associated antigen. *Cancer Res.* 40: 3147–3154.
- Ritz, J., J. M. Pesando, S. E. Sallan, L. A. Clavell, J. Notis-McConarty, P. Rosenthal, and S. F. Schollossman. 1981. Serotherapy of acute lymphoblastic leukemia with monoclonal antibody. *Blood* 58: 141–152.
- Bertram, J. H., P. S. Gill, A. M. Levine, D. Boquiren, F. M. Hoffman, P. Meyer, and M. S. Mitchell. 1986. Monoclonal antibody T101 in T cell malignancies: a clinical, pharmacokinetic, and immunologic correlation. *Blood* 68: 752–761.
- Gruber, R., E. Holz, and G. Riethmuller. 1996. Monoclonal antibodies in cancer therapy. *Springer Semin. Immunopathol.* 18: 243–251.
- Glennie, M., and P. Johnson. 2000. Clinical trials of antibody therapy. *Immunol. Today* 21: 403–410.
- Carter, P. 2001. Improving the efficacy of antibody-based cancer therapies. *Nature* 1: 118–129.

7. Stern, M., and R. Herrmann. 2005. Overview of monoclonal antibodies in cancer therapy: present and promise. *Crit. Rev. Oncol. Hematol.* 54: 11–29.
8. Jurianz, K., S. Ziegler, H. Garcia-Schuler, S. Kraus, O. Bohana-Kashtan, Z. Fishelson, and M. Kirschfink. 1999. Complement resistance of tumor cells: basal and induced mechanisms. *Mol. Immunol.* 36: 929–939.
9. Johnson, P., and M. Glennie. 2003. The mechanisms of action of rituximab in the elimination of tumor cells. *Semin. Oncol.* 30: 3–8.
10. Di Gaetano, N., E. Cittera, R. Nota, A. Vecchi, V. Grieco, E. Scanziani, M. Botto, M. Intron, and J. Golay. 2003. Complement activation determines the therapeutic activity of rituximab in vivo. *J. Immunol.* 171: 1581–1587.
11. Fishelson, Z., N. Donin, S. Zell, S. Schultz, and M. Kirschfink. 2004. Obstacles to cancer immunotherapy: expression of membrane complement regulatory proteins (mCRPs) in tumors. *Mol. Immunol.* 40: 109–123.
12. Hong, F., J. Yan, J. T. Baran, D. J. Allendorf, R. D. Hansen, G. R. Ostroff, P. X. Xing, N. V. Cheung, and G. D. Ross. 2004. Mechanism by which orally administered β -1,3-glucans enhance the tumoricidal activity of antitumor monoclonal antibodies in murine tumor models. *J. Immunol.* 173: 797–806.
13. Teeling, J., R. R. French, M. S. Cragg, J. van den Brakel, M. Pluyter, H. Huang, C. Chan, P. W. Parren, C. E. Hack, M. Dechant, et al. 2004. Characterization of new human CD20 monoclonal antibodies with potent cytolytic activity against non-Hodgkin's lymphomas. *Blood* 104: 1793–1800.
14. Taylor, R. P. 2005. Use of biological response modifiers to enhance the action of rituximab. *Leuk. Res.* 29: 599–600.
15. Clynes, R. A., T. L. Towers, L. G. Presta, and J. V. Ravetch. 2000. Inhibitory Fc receptors modulate in vivo cytotoxicity against tumor targets. *Nat. Med.* 6: 443–446.
16. Hernandez-Ilizaliturri, F. J., V. Jupudy, J. Ostberg, E. Oflazoglu, A. Huberman, E. Repasky, and M. S. Czuczman. 2003. Neutrophils contribute to the biological antitumor activity of rituximab in a non-Hodgkin's lymphoma severe combined immunodeficiency mouse model. *Clin. Cancer Res.* 9: 5866–5873.
17. Uchida, J., Y. Hamaguchi, J. A. Oliver, J. V. Ravetch, J. C. Poe, K. M. Haas, and T. F. Tedder. 2004. The innate mononuclear phagocyte network depletes B lymphocytes through Fc receptor-dependent mechanisms during anti-CD20 antibody immunotherapy. *J. Exp. Med.* 199: 1659–1669.
18. Hamaguchi, Y., J. Uchida, D. W. Cain, G. M. Venturi, J. C. Poe, K. M. Haas, and T. F. Tedder. 2005. The peritoneal cavity provides a protective niche for B1 and conventional B lymphocytes during anti-CD20 immunotherapy in mice. *J. Immunol.* 174: 4389–4399.
19. Letvin, N. L., J. Ritz, L. J. Guida, J. M. Yetz, J. M. Lambert, E. L. Reinherz, and S. F. Schlossman. 1985. In vivo administration of lymphocyte-specific monoclonal antibodies in nonhuman primates. I. Effects of anti-T11 antibodies on the circulating T cell pool. *Blood* 66: 961–966.
20. Miller, R. A., D. G. Maloney, J. McKillop, and R. Levy. 1981. In vitro effects of murine hybridoma monoclonal antibody in a patient with T-cell leukemia. *Blood* 58: 78–86.
21. Schroff, R. W., R. A. Klein, M. M. Farrell, and H. C. Stevenson. 1984. Enhancing effects of monoclonal antibodies on modulation of a lymphocyte membrane antigen. *J. Immunol.* 133: 2270–2277.
22. Schroff, R. W., M. M. Farrell, R. A. Klein, H. C. Stevenson, and N. L. Warner. 1985. Induction and enhancement by monoclonal antibodies of antibody-induced modulation of a variety of human lymphoid cell surface antigens. *Blood* 66: 620–626.
23. Davis, W., P. T. Harrison, M. J. Hutchinson, and J. M. Allen. 1995. Two distinct regions of Fc γ RI initiate separate signalling pathways involved in endocytosis and phagocytosis. *EMBO J.* 14: 432–441.
24. Lovdal, T., E. Andersen, and A. B. T. Brech. 2000. Fc receptor mediated endocytosis of small soluble immunoglobulin G immune complexes in Kupffer and endothelial cells from rat liver. *J. Cell Sci.* 113: 3255–3266.
25. Stuart, L. M., and R. A. B. Ezekowitz. 2005. Phagocytosis: elegant complexity. *Immunology* 22: 539–550.
26. Maloney, D. G., A. J. Grillo-López, C. A. White, D. Bodkin, R. J. Schilder, J. A. Neidhart, N. Janakiraman, K. A. Foon, T. Liles, B. K. Dallaré, et al. 1997. IDEC-C2B8 (rituximab) anti-CD20 monoclonal antibody therapy in patients with relapsed low-grade non-Hodgkin's lymphoma. *Blood* 90: 2188–2195.
27. McLaughlin, P., A. J. Grillo-Lopez, B. K. Link, R. Levy, M. S. Czuczman, M. E. Williams, M. R. Heyman, I. Bence-Bruckler, C. A. White, F. Cabanillas, et al. 1998. Rituximab chimeric anti-CD20 monoclonal antibody therapy for relapsed indolent lymphoma: half of patients respond to a four-dose treatment program. *J. Clin. Oncol.* 16: 2825–2833.
28. McLaughlin, P. 2001. Rituximab: perspective on single agent experience, and future directions in combination trials. *Crit. Rev. Oncol. Hematol.* 40: 3–16.
29. Coiffier, B., E. Lepage, J. Briere, R. Herbrecht, H. Tilly, R. Bouabdallah, P. Morel, E. Van Den Neste, G. Salles, P. Gaulard, et al. 2002. CHOP chemotherapy plus rituximab compared with CHOP alone in elderly patients with diffuse large-B-cell lymphoma. *N. Engl. J. Med.* 346: 235–242.
30. Smith, M. R. 2003. Rituximab (monoclonal anti-CD20 antibody): mechanisms of action and resistance. *Oncogene* 22: 7359–7368.
31. Maloney, D. G. 2005. Concepts in radiotherapy and immunotherapy: anti-CD20 mechanisms of action and targets. *Semin. Oncol.* 32: S19–S26.
32. Cragg, M. S., C. A. Walshe, A. O. Ivanov, and M. J. Glennie. 2005. The biology of CD20 and its potential as a target for mAb therapy. *Curr. Dir. Autoimmun.* 8: 140–174.
33. Gopal, A. K., and O. W. Press. 1999. Clinical applications of anti-CD20 antibodies. *J. Lab. Clin. Med.* 134: 445–450.
34. Kennedy, A. D., P. V. Beum, M. D. Solga, D. J. DiLillo, M. A. Lindorfer, C. E. Hess, J. J. Densmore, M. E. Williams, and R. P. Taylor. 2004. Rituximab infusion promotes rapid complement depletion and acute CD20 loss in chronic lymphocytic leukemia. *J. Immunol.* 172: 3280–3288.
35. Tsuchiya, S., M. Yamabe, Y. Yamaguchi, Y. Kobayashi, T. Konno, and D. Tada. 1980. Establishment and characterization of a human acute monocytic leukemia cell line (THP-1). *Int. J. Cancer* 26: 171–176.
36. Nakamura, T., H. Hemmi, H. Aso, and N. Ishida. 1986. Variants of a human monocytic leukemia cell line (THP-1): induction of differentiation by retinoic acid, interferon- γ , and T-lymphocyte-derived differentiation-inducing activity. *J. Natl. Cancer Inst.* 77: 21–27.
37. Schwende, H., E. Fitzke, P. Ambs, and P. Dieter. 1996. Differences in the state of differentiation of THP-1 cells induced by phorbol ester and 1,25-dihydroxyvitamin D₃. *J. Leukocyte Biol.* 59: 555–561.
38. Huhn, D., C. von Schilling, M. Wilhelm, A. Ho, M. Hallek, R. Kuse, W. Knauf, U. Riedel, A. Hinke, S. Srock, et al. 2001. Rituximab therapy of patients with B-cell chronic lymphocytic leukemia. *Blood* 98: 1326–1331.
39. Kennedy, A. D., M. D. Solga, T. A. Schuman, A. W. Chi, M. A. Lindorfer, W. M. Sutherland, P. L. Foley, and R. P. Taylor. 2003. An anti-C3b(i) mAb enhances complement activation, C3b(i) deposition, and killing of CD20⁺ cells by rituximab. *Blood* 101: 1071–1079.
40. Craig, M. L., A. J. Bankovich, and R. P. Taylor. 2002. Visualization of the transfer reaction: tracking immune complexes from erythrocyte complement receptor 1 to macrophages. *Clin. Immunol.* 105: 36–47.
41. Estrov, Z., M. Talpaz, S. Ku, D. Harris, Q. Van, M. Beran, C. Hirsch-Ginsberg, Y. Huh, G. Yee, and R. Kurzrock. 1998. Z-138: a new mature B-cell acute lymphoblastic leukemia cell line from a patient with transformed chronic lymphocytic leukemia. *Leuk. Res.* 22: 341–353.
42. Lindorfer, M. A., H. B. Jinivizian, P. L. Foley, A. D. Kennedy, M. D. Solga, and R. P. Taylor. 2003. The B cell complement receptor 2 transfer reaction. *J. Immunol.* 170: 3671–3678.
43. Clarkson, S. B., R. P. Kimberley, J. E. Valinsky, M. D. Witmer, J. B. Bussel, R. L. Nachman, and J. C. Unkeless. 1986. Blockade of clearance of immune complexes by an anti-Fc γ receptor monoclonal antibody. *J. Exp. Med.* 164: 474–489.
44. Kurosaka, K., N. Watanabe, and Y. Kobayashi. 1998. Production of proinflammatory cytokines by phorbol myristate acetate-treated THP-1 cells and monocyte-derived macrophages after phagocytosis of apoptotic CTLL-2 cells. *J. Immunol.* 161: 6245–6249.
45. Lee-MacAry, A. E., E. L. Ross, D. Davies, R. Laylor, J. Honeychurch, M. J. Glennie, D. Snary, and R. W. Wilkinson. 2001. Development of a novel flow cytometric cell-mediated cytotoxicity assay using the fluorophores PKH-26 and TO-PRO-3 iodide. *J. Immunol. Methods* 252: 83–92.
46. Hoppner, M., J. Luhm, P. Schlenke, P. Koritke, and C. Fronh. 2002. A flow-cytometry based cytotoxicity assay using stained effector cells in combination with native target cells. *J. Immunol. Methods* 267: 157–163.
47. Herre, J., A. S. J. Marshall, E. Caron, A. D. Edwards, D. L. Williams, E. Schweighoffer, V. Tybulewicz, C. Reis e Sousa, S. Gordon, and G. D. Brown. 2004. Dectin-1 uses novel mechanisms for yeast phagocytosis in macrophages. *Blood* 104: 4038–4045.
48. Roy, R., U. M. Wewer, D. Zurakowski, S. E. Pories, and M. A. Moses. 2004. ADAM 12 cleaves extracellular matrix proteins and correlates with cancer status and stage. *J. Biol. Chem.* 279: 51323–51330.
49. Martinez-Climent, J. A., E. Vizcarra, D. Sanchez, D. Blesa, I. Marugan, I. Benet, F. Sole, F. Rubio-Moscardo, M. J. Terol, J. Climent, et al. 2001. Loss of a novel tumor suppressor gene locus at chromosome 8p is associated with leukemic mantle cell lymphoma. *Blood* 98: 3479–3482.
50. De Leeuw, R. J., J. J. Davies, A. Rosenwald, G. Bebb, R. D. Gascoyne, M. J. S. Dyer, L. M. Staudt, J. A. Martinez-Climent, and W. L. Lam. 2004. Comprehensive whole genome array CGH profiling of mantle cell lymphoma model genomes. *Hum. Mol. Genet.* 13: 1827–1837.
51. DiLillo, D. J., A. W. Pawluczko, W. Peng, A. D. Kennedy, P. V. Beum, M. A. Lindorfer, and R. P. Taylor. 2006. Selective and efficient inhibition of the alternative pathway of complement by a mAb that recognizes C3b/iC3b. *Mol. Immunol.* 43: 1010–1019.
52. Cardarelli, P. M., M. Quinn, D. Buckman, Y. Fang, D. Colcher, D. King, C. Bebbington, and G. Yarranton. 2002. Binding to CD20 by anti-B1 antibody or F(ab')₂ is sufficient for induction of apoptosis in B-cell lines. *Cancer Immunol. Immunother.* 51: 15–24.
53. Craig, M. L., A. J. Bankovich, J. McElhenney, and R. P. Taylor. 2000. Clearance of anti-double-stranded DNA antibodies: the natural immune complex clearance mechanism. *Arthritis Rheum.* 43: 2265–2275.
54. Munn, D. H., and N.-K. V. Cheung. 1990. Phagocytosis of tumor cells by human monocytel cultured in recombinant macrophage colony-stimulated factor. *J. Exp. Med.* 172: 231–237.
55. Wallace, P. K., P. Kaufman, L. Lewis, T. Keler, A. Givan, J. Fisher, M. Waugh, A. Wahner, P. Guyre, M. Fanger, and M. Ernstoff. 2001. Bispecific antibody-targeted phagocytosis of HER-2/neu expressing tumor cells by myeloid cells activated in vivo. *J. Immunol. Methods* 248: 167–182.
56. Taylor, R. P., A. W. Pawluczko, P. V. Beum, A. D. Kennedy, M. A. Lindorfer, J. J. Densmore, J. Eggleton, K. L. LoRusso, and M. E. Williams. 2004. A pilot study of thrice-weekly low dose rituximab (RTX) in the treatment of chronic lymphocytic leukemia (CLL) suggests enhanced therapeutic targeting compared to standard dose regimens. *Blood* 104: 691a.
57. Lambiris, J. D., A. Sahu, and R. A. Wetzel. 1998. The chemistry and biology of C3, C4 and C5. In *The Human Complement System in Health and Disease*. J. E. Volanakis and M. M. Frank, eds. Marcel Dekker, New York, pp. 83–119.
58. Lutz, H. U., P. Stammer, E. Jelezarova, M. Nater, and P. Spath. 1996. High doses of immunoglobulin G attenuate immune aggregate-mediated complement activation by enhancing physiologic cleavage of C3b in C3b-IgG complexes. *Blood* 88: 184–193.

59. Kishore, U., and K. B. Reid. 2000. C1q: structure, function, and receptors. *Immunopharmacology* 49: 159–170.
60. Stokol, T., P. O'Donnell, L. Xiao, S. Knight, G. Stavarakis, M. Botto, U. H. von Andrian, and T. N. Mayadas. 2004. C1q governs deposition of circulating immune complexes and leukocyte Fc γ receptors mediate subsequent neutrophil recruitment. *J. Exp. Med.* 200: 835–846.
61. Lutz, H., P. Stammler, and S. Fasler. 1993. Preferential formation of C3b-IgG complexes in vitro and in vivo from nascent C3b and naturally occurring antibody 3 antibodies. *J. Biol. Chem.* 268: 17418–17426.
62. Cragg, M. S., and M. J. Glennie. 2004. Antibody specificity controls in vivo effector mechanisms of anti-CD20 reagents. *Blood* 103: 2738–2743.
63. Shen, L., R. F. Graziano, and M. W. Fanger. 1989. The functional properties of Fc γ RI, II and III on myeloid cells: a comparative study of killing of erythrocytes and tumor cells mediated through the different Fc receptors. *Mol. Immunol.* 26: 959–969.
64. Fleit, H. B., and C. D. Kobasiuk. 1991. The human monocyte-like cell line THP-1 expresses Fc γ RI and Fc γ RII. *J. Leukocyte Biol.* 49: 556–565.
65. Espinosa, E., J. Tabiasco, D. Hudrisier, and J. J. Fournie. 2002. Synaptic transfer by human $\gamma\delta$ T cells stimulated with soluble or cellular antigens. *J. Immunol.* 168: 6336–6343.
66. Berton, G., A. Mocsai, and C. A. Lowell. 2005. Src and Syk kinases: key regulators of phagocytic cell activation. *Trends Immunol.* 26: 208–214.
67. Tabiasco, J., A. Vercellone, F. Meggetto, D. Hudrisier, P. Brousset, and J. J. Fournie. 2003. Acquisition of viral receptor by NK cells through immunological synapse. *J. Immunol.* 170: 5993–5998.
68. Poupot, M., F. Pont, and J. J. Fournie. 2005. Profiling blood lymphocyte interactions with cancer cells uncovers the innate reactivity of human $\gamma\delta$ T cells to anaplastic large cell lymphoma. *J. Immunol.* 174: 1717–1722.
69. Tabiasco, J., E. Espinosa, D. Hudrisier, E. Joly, J. J. Fournie, and A. Vercellone. 2002. Active trans-synaptic capture of membrane fragments by natural killer cells. *Eur. J. Immunol.* 32: 1502–1508.
70. Bauvois, B., J. Sanceau, and J. Wietzerbin. 1992. Human U937 cell surface peptidase activities: characterization and degradative effect on tumor necrosis factor- α . *Eur. J. Immunol.* 22: 923–930.
71. Bazil, V., and J. L. Strominger. 1994. Metalloprotease and serine proteases are involved in cleavage of CD43, CD44, and CD16 from stimulated human granulocytes. *J. Immunol.* 152: 1314–1322.
72. Edwards, J. C. W., M. J. Leandro, and G. Cambridge. 2005. B lymphocyte depletion in rheumatoid arthritis: targeting of CD20. *Curr. Dir. Autoimmun.* 8: 175–192.
73. Looney, R. J., J. Anolik, and I. Sanz. 2005. Treatment of SLE with anti-CD20 monoclonal antibody. *Curr. Dir. Autoimmun.* 8: 193–205.
74. Treon, S. P., M. Hansen, A. R. Branagan, S. Verselis, C. Emmanouilides, E. Kimby, S. R. Frankel, N. Touroutoglou, B. Turnbull, K. C. Anderson, et al. 2005. Polymorphisms in Fc γ RIIIA (CD16) receptor expression are associated with clinical response to rituximab in Waldenstrom's macroglobulinemia. *J. Clin. Oncol.* 23: 474–481.
75. Weng, W. K., and R. Levy. 2003. Two immunoglobulin G fragment C receptor polymorphisms independently predict response to Rituximab in patients with follicular lymphoma. *J. Clin. Oncol.* 21: 3940–3947.
76. Cartron, G., L. Dacheux, G. Salles, P. Solal-Celigny, P. Bardos, P. Colombat, and H. Watier. 2002. Therapeutic activity of humanized anti-CD20 monoclonal antibody and polymorphism in IgG Fc receptor Fc γ RIIIa gene. *Blood* 99: 754–758.
77. Foran, J. M., A. J. Norton, I. N. M. Micallef, D. C. Taussig, J. A. L. Amess, A. Z. S. Rohatiner, and T. A. Lister. 2001. Loss of CD20 expression following treatment with rituximab (chimaeric monoclonal anti-CD20): a retrospective cohort analysis. *Br. J. Haematol.* 114: 881–883.
78. Pickartz, T., F. Ringel, M. Wedde, H. Renz, A. Klein, N. von Neuhoff, P. Dreger, K. A. Kreuzer, C. A. Schmidt, S. Srock, et al. 2001. Selection of B-cell chronic lymphocytic leukemia cell variants by therapy with anti-CD20 monoclonal antibody rituximab. *Exp. Hematol.* 29: 1410–1416.
79. Harrison, P. T., W. Davis, J. C. Norman, A. R. Hockaday, and J. M. Allen. 1994. Binding of monomeric immunoglobulin G triggers Fc γ RI-mediated endocytosis. *J. Biol. Chem.* 269: 24396–24402.
80. Rinnooy Kan, E. A., E. Platzer, K. Welte, and C. Y. Wang. 1984. Modulation induction of the T3 antigen by OKT3 antibody is monocyte dependent. *J. Immunol.* 133: 2979–2985.
81. Van der Velden, V. H. J., J. G. te Marvelde, P. G. Hoogeveen, I. D. Bernstein, A. B. Houtsmuller, M. S. Berger, and J. J. M. van Dongen. 2001. Targeting of the CD33-calicheamicin immunoconjugate Mylotarg (CMA-676) in acute myeloid leukemia: in vivo and in vitro saturation and internalization by leukemic and normal myeloid cells. *Blood* 97: 3197–3204.
82. Chatenoud, L., M. F. Baudrihaye, H. Kreis, G. Goldstein, J. Schindler, and J. F. Bach. 1982. Human in vivo antigenic modulation induced by the anti-T cell OKT3 monoclonal antibody. *Eur. J. Immunol.* 12: 979–982.
83. Pesando, J. M., P. Hoffman, and M. Abed. 1986. Antibody-induced antigenic modulation is antigen dependent: characterization of 22 proteins on a malignant human B cell line. *J. Immunol.* 137: 3689–3695.
84. Manske, J. M., D. J. Buchsbaum, S. M. Azemove, D. E. Hanna, and D. A. Vallera. 1986. Antigenic modulation by anti-CD5 immunotoxins. *J. Immunol.* 136: 4721–4728.
85. Kreitman, R., W. Wilson, K. Bergeron, K. Raggio, M. Stetler-Stevenson, D. Fitzgerald, and I. Pastan. 2001. Efficacy of the anti-CD22 recombinant immunotoxin BL22 in chemotherapy-resistant hairy-cell leukemia. *N. Engl. J. Med.* 345: 241–247.
86. Rajvanshi, P., H. M. Shulman, E. L. Sievers, and G. B. McDonald. 2002. Hepatic sinusoidal obstruction after gemtuzumab ozogamicin (mylotarg) therapy. *Blood* 99: 2310–2314.
87. Farag, S. S., I. W. Flinn, R. Modali, T. A. Lehman, D. Young, and J. C. Byrd. 2004. Fc γ RIIIa and Fc γ RIIa polymorphisms do not predict response to rituximab in B-cell chronic lymphocytic leukemia. *Blood* 103: 1472–1474.